J Mater Sci: Mater Electron (2023)34:1104

Modification of free-volume defects in the GaS_2–Ga_2S_3–CsCl glasses

H. Klym[1,2,*], L. Calvez[3], and A. I. Popov[4]

[1] *Lviv Polytechnic National University, 12 Bandera Str., Lviv 79013, Ukraine*
[2] *Ivan Franko National University of Lviv, 50 Drahomanova Str., Lviv 79005, Ukraine*
[3] *Equipe Verres et Céramiques, Institute des Sciences chimiques de Rennes, UMR-CNRS 6226, Université de Rennes 1, 35042 Rennes Cedex, France*
[4] *Institute of Solid State Physics, University of Latvia, Kengaraga 8, 1063 Riga, Latvia*

Received: 11 January 2023
Accepted: 7 April 2023

ABSTRACT

Modification of free-volume positron trapping defects in the GaS_2–Ga_2S_3–CsCl chalcogenide glasses was studied using positron annihilation lifetime spectroscopy and Doppler broadening of annihilation radiation methods. It is shown that the addition of CsCl to the main glass matrix leads to agglomeration of internal free-volume defects, which are di- or tri-atomic vacancies. However, an excessive amount of CsCl component causes a decrease in the size and content of these defects in the internal structure of the glass against the background of water adsorption in nanovoids with a radius of 0.3 nm. The obtained results are confirmed by normal and abnormal trends in the correlation of the *S* parameter, which characterizes the annihilation of positrons with low-momentum valence electrons and the *W* parameter, which corresponds to the annihilation of positrons with high-momentum core electrons.

1 Introduction

Development of IR photonics has posed a problem of finding new functional media for the efficient transmission of electromagnetic radiation of a wide spectral range, as well as the production of technologies for various instrument applications including sensors, optical waveguides, fibers, resonators, detectors, amplifiers, signal converters, etc. [1–6]. Significant successes in this field are associated with the possibility of chemical–technological modification of elements based on chalcogenide glasses GeS_2–Ga_2S_3 through components that give new properties [7–11]. Thus, the basic functionality of glasses can be effectively combined with the high transparency of halides in the visible part of the spectrum, creating mixed chalcogenide–halide glasses [12–15]. The combination of optical properties with flexibility in the choice of composition and synthesis technology makes it indispensable in photonics.

Finding the best glass compositions for practical applications is very important today. There are two alternative ways to solve this problem. The first consists in the expansion of compositions due to the

Address correspondence to E-mail: halyna.i.klym@lpnu.ua; klymha@yahoo.com

https://doi.org/10.1007/s10854-023-10431-9
Published online: 06 May 2023

change in the synthesis technology regarding the mode of cooling, the melt, and the initial chemical components [16]. Unfortunately, such chemical and technological modification is extensive. A more effective solution to this problem is the structural modification of known compositions of chalcogenide glasses (in addition to external factors) by adding additional components to the main matrix, which makes it possible to obtain a material with predetermined physical properties and enhanced functionality [17, 18].

Thus, the addition of CsCl alkaline halides to GeS_2–Ga_2S_3 glass leads not only to a change in their optical properties [19, 20], but will also affect the redistribution of internal free volume, modification of defects and nanovoids in the internal structure of the glassy matrix. However, the structure of such modified glasses associated with free-volume defects has not been fully investigated in all aspects of its manifestation, which significantly limits further progress in modern IR photonics. It is known that the closest arrangement of atoms in glass and nanomaterials can be adequately investigated using numerous experimental measurement methods [21–32]. However, the row of experimental probes available to study atomic-deficient void structure of such materials is rather limited, especially at nanometer and subnanometer scale. In this work, we used alternative methods of positron annihilation lifetime (PAL) spectroscopy and Doppler broadening of annihilation line (DBAL) [33, 34] to study free-volume defects in the GaS_2–Ga_2S_3–CsCl chalcogenide glasses.

In our previous research, we studied changes in the structure of the free volume of Ge–Ga–Se/S chalcogenide glass under the influence of thermal treatment [35, 36], changes in matrix components [37, 38], etc. For the analysis of PAL spectra, decomposition into two or three components was used. It was shown that additional influences cause the processes of agglomeration and fragmentation of free-volume voids [37]. In this work, the modification of free-volume defects in the $(80GeS_2–20Ga_2S_3)_{100-x}(CsCl)_x$ glasses with the addition of different amounts of CsCl (x = 0, 5, 10, 15) is investigated. The studied PAL spectra were analyzed by splitting into two and three components to maximize the detection of all possible processes that occur in the internal free-volume structure of glasses, as well as the expansion and clarification of our previous studies.

2 Experimental

Samples of the base $80GeS_2$–$20Ga_2S_3$ glasses and glasses with the addition of CsCl ($80GeS_2$–$20Ga_2S_3$–CsCl) were obtained by fusing a mixture of high-purity Ge, Ga, S materials (previously purified by dynamic distillation) and CsCl in a sealed quartz ampoule in a vacuum under a pressure of 10^{-4} mbar [38–40]. The raw from the starting materials was heated to 850 °C and kept at this temperature for 8 h to complete the reaction and avoid explosion due to the high vapor pressure. After that the quartz tube was cooled in water at room temperature, annealed at a temperature close to the glass transition temperature T_g for 3 h to reduce internal stresses and slowly cooled at room temperature. This material is also characterized by the limitation of the glass transition zone within the framework of pseudo-twin GeS_2–Ga_2S_3–CsCl systems [39]. The physical properties of the obtained $(80GeS_2–20Ga_2S_3)_{100-x}(CsCl)_x$, x = 0, 5, 10, 15 glasses and their elemental composition are shown in Tables 1 and 2, respectively. The error bar for experimentally determined numerical values were 0.01. The density was determined according to Archimedes' method [41].

As can be seen from Table 1, the addition of CsCl to the base $80GeS_2$–$20Ga_2S_3$ glass leads to a significant decrease in their glass transition temperature T_g, while the crystallization temperature T_x remains practically unchanged regardless of the CsCl content. Therefore, the $\Delta T = T_x - T_g$ parameter was used to estimate the thermal stability of glasses caused by the introduction of CsCl and to achieve the maximum for individual composites, for example, $(80GeS_2–20Ga_2S_3)_{85}(CsCl)_{15}$. The introduction of chloride into the composition of the base glass causes the destruction of Ge−S or Ga−S bonds and the formation of $GaS_{3/2}Cl^-$ tetrahedra [39]. In this case, Ga remains four-coordinated [42], but the degree of connectivity of lattice glass nodes decreases. On the other hand, the formation of this complex of anions contributes to the formation of glasses. The density of $(80GeS_2–20Ga_2S_3)_{100-x}(CsCl)_x$, x = 0, 5, 10, 15 glasses increases with CsCl content, which is due to the large atomic mass of Cs.

For convenience, the studied $(80GeS_2–20Ga_2S_3)_{100}(CsCl)_0$, $(80GeS_2–20Ga_2S_3)_{95}(CsCl)_5$, $(80GeS_2–20Ga_2S_3)_{90}(CsCl)_{10}$, and $(80GeS_2–20Ga_2S_3)_{85}(CsCl)_{15}$ glasses are denoted as $(CsCl)_0$, $(CsCl)_5$, $(CsCl)_{10}$, and $(CsCl)_{15}$, respectively.

Table 1 Physical properties of the $(80GeS_2– 20Ga_2S_3)_{100-x}(CsCl)_x$, x = 0, 5, 10, 15 glasses

Glass composition	T_g(°C) [39]	T_x(°C) [39]	ΔT (°C) [39]	(g/cm^3) [39]	V_m (cm^3/mol) [39]
$(80GeS_2–20Ga_2S_3)_{100}(CsCl)_0$	442	520	78	2.932	54.45
$(80GeS_2–20Ga_2S_3)_{95}(CsCl)_5$	416	532	116	2.954	53.61
$(80GeS_2–20Ga_2S_3)_{90}(CsCl)_{10}$	396	526	130	2.966	53.32
$(80GeS_2–20Ga_2S_3)_{85}(CsCl)_{15}$	378	521	143	2.972	53.20

Table 2 Elemental composition of $(80GeS_2–20Ga_2S_3)_{100-x}(CsCl)_x$, x = 0, 5, 10, and 15 glasses

Glass composition	Theoretical stoichiometric composition	Experimentally determined elemental composition of glasses				
		Ge	Ga	S	Cs	Cl
$(80GeS_2–20Ga_2S_3)_{100}(CsCl)_0$	$Ge_{23.53}Ga_{11.76}S_{64.71}$	22.18	11.70	66.12	0	0
$(80GeS_2–20Ga_2S_3)_{95}(CsCl)_5$	$Ge_{23.17}Ga_{11.59}S_{63.72}CsCl_{1.52}$	28.48	10.97	63.53	1.38	1.65
$(80GeS_2–20Ga_2S_3)_{90}(CsCl)_{10}$	$Ge_{22.79}Ga_{11.39}S_{62.66}CsCl_{3.16}$	21.11	10.46	62.51	2.95	2.97
$(80GeS_2–20Ga_2S_3)_{85}(CsCl)_{15}$	$Ge_{22.37}Ga_{11.18}S_{61.51}CsCl_{4.93}$	20.89	10.41	59.56	4.39	4.74

The study of modification of free-volume defects in glasses caused by introduction of different amounts of CsCl into the initial matrix was carried by PAL method [35–39]. Experimental PAL spectra were obtained using the ORTEC system with a resolution of 230 ps at temperature of 22 °C and relative humidity of 35%, provided by a special installation [35–39]. Two identical glass samples were placed on both sides of the positron source (isotope^{22} Na with an activity of $\sim$ 50 kBq).

The measured PAL spectra were processed by the specially developed program LT 9.0 [43] using two- and three-component fitting decomposition, since for these chalcogenide glasses both cases are possible taking into account the optimal value of the fitting parameters [36]. In addition, parameters such as the average positron lifetime τ_{av}, the positron lifetime in the defect-free volume τ_b, the positron trapping rate in defects κ_d were calculated within the framework of two-state positron trapping model in free-volume defects [44]. The resulting inaccuracies in positron lifetimes τ and intensities I were $\pm$ 0.002 ns and $\pm$ 1% ($\pm$ 0.1% for I_3), respectively, which led to $\pm$ 0.01 ns^{-1} error-bar in positron trapping rate of defects κ_d.

In addition to PAL methods, the experimental system for measuring the Doppler broadening of annihilation line (DBAL) was set up in a PAL geometry using a high-purity Ge detector with an energy resolution of 1.54 keV at 511 keV. The shape of the 511 keV annihilation line was considered in terms of the so-called S and W parameters [35, 45]. The S parameter characterizes the annihilation of positrons with low-momentum valence electrons sensitive mainly to defects in the free volume. The W parameter corresponds to the annihilation of positrons with high-momentum core electrons, which are sensitive mainly to the chemical environment at the annihilation site. For the DBAL spectrum the energy range of the $S-W$ parameterization was selected from 502.29 to 519.71 keV [35]. Since S parameter was chosen close to a reference value of $\sim$ 0.5 in DBAL measurements, it could not be determined better accuracy than $\pm$ 0.0015. The accuracy of determining the parameter W was $\pm$ 0.0002.

3 Results and discussion

By introducing different amounts of CsCl into the base $80GeS_2–20Ga_2S_3$ glass matrix it is logical to assume that their content will modify the free-volume defects in the glasses. Changes in the internal free volume will be reflected in the parameters of positron trapping in defects obtained within PAL method.

For a general assessment of the transformations of free volumes in the $80GeS_2–20Ga_2S_3$–CsCl glasses, the PAL spectra were initially decomposed into two components with $_1$ and $_2$ lifetimes and I_1 and I_2 intensities within the framework of two-state

positron trapping model [44] as for typical chalcogenide glasses [33]. The dependences of fitting parameters and positron trapping modes parameters from CsCl content for $(CsCl)_0$, $(CsCl)_5$, $(CsCl)_{10}$ and $(CsCl)_{15}$ glasses are shown in Fig. 1.

As noted in our previous work [35–38], the first component (τ_1, I_1) of the breakdown of PAL spectrum for chalcogenide glasses has no physical meaning. Therefore, the main attention will be focused on the analysis of the second defect-related component (τ_2, I_2). As can be seen from Fig. 1 an increase in CsCl content in the base $80GeS_2$–$20Ga_2S_3$ glass leads to a significant increase in the lifetime τ_2 [from 0.429 ns for $(CsCl)_5$ to 0.501 ns for glasses $(CsCl)_{10}$] and a decrease in the intensity I_2 from 0.38 to 0.27. Such changes in the parameters of the second component testify to the obvious processes of agglomeration of internal free-volume defects caused by the appearance and increase of CsCl in the structure of GeS_2–Ga_2S_3 glasses. Average lifetime τ_{av} and the lifetime $_b$ correlates with the changes in the fitting parameters.

The atomic compaction of the structure of GeS_2–Ga_2S_3 basic glasses, caused by the presence of CsCl, is most significantly reflected in the positron trapping rate in defects κ_d. The value of this parameter decreases from 1.01 to 0.72 ns^{-1} with the appearance of CsCl in the $80GeS_2$–$20Ga_2S_3$ glasses. A further increase in CsCl is accompanied by a decrease in κ_d to 0.59 ns^{-1} (for $(CsCl)_{15}$). The obtained values for positron trapping modes make it possible to assert that positron trapping centers are rather of the same type, being most probably as di- or tri-atomic vacancies.

The results obtained by PAL method are in good agreement with the DRAL studies presented in the form of correlation dependences of *S*–*W* parameters (Fig. 2). Although only two measurements were made for four different $(CsCl)_0$, $(CsCl)_5$, $(CsCl)_{10}$, and $(CsCl)_{15}$ glass compositions, it can be stated that the evolution of the *S*–*W* parameters is linear in the direction of decreasing *S* and increasing *W* for the initial $(CsCl)_0$ glasses (with atomic density

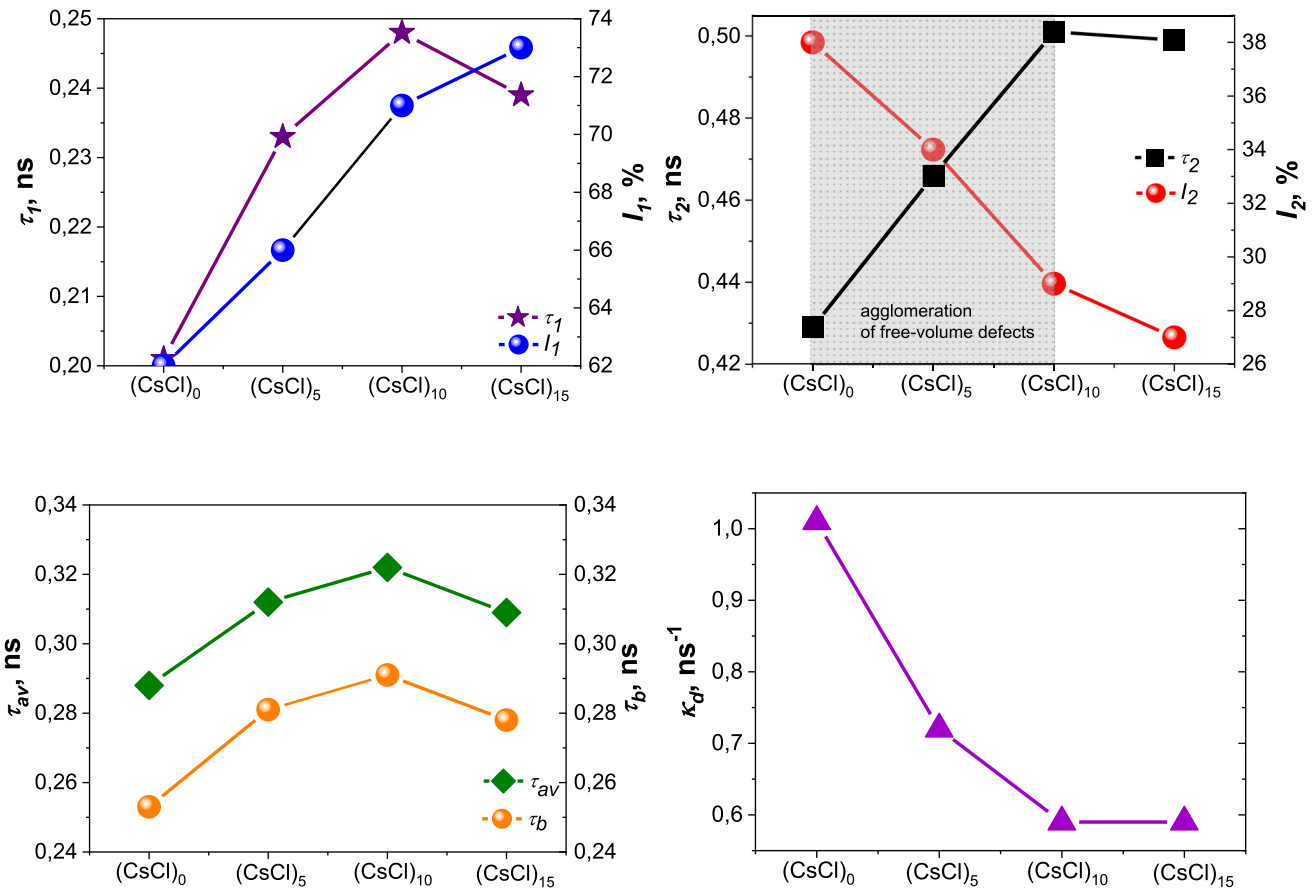

Fig. 1 Dependences of fitting parameters and positron trapping modes for the $80GeS_2$–$20Ga_2S_3$–CsCl glasses calculated within two-components fitting procedure

ρ = 2.932 g/cm^3) as well as $(CsCl)_{10}$ and $(CsCl)_{15}$ samples (with atomic density 2.954 and 2.966 g/cm^3, respectively).

This behavior as in the case of crystallization processes at the initial stages in $80GeSe_2$–$20Ga_2Se_3$ glasses [35] corresponds to the normal trend in the change of *S*–*W* parameters, when the total free-volume traps (defects) where positrons are captured is mainly accompanied by atomic compaction samples (the positron trapping rate by defects κ_d decreases and the atomic density ρ increases). The normal trend in the correlation of the $\kappa_{d\text{-}\rho}$ parameters demonstrates the agglomeration of free-volume defects with increasing of CsCl in the structure of GeS_2–Ga_2S_3 glasses.

An exception is the $(CsCl)_{15}$ glass, which is characterized by an anomalous trend in the evolution of *S*–*W* parameters (Fig. 2) that manifests itself as a deviation from linearity. An explanation for this deviation can be given using the decomposition of the PAL spectra into three components.

In addition, in order to study the evolution of free-volume defects and nanovoids in glasses caused by the modification by CsCl, PAL studies were carried out with decomposition into three components with τ_1, τ_2, τ_3 lifetimes and I_1, I_2, I_3 intensities. As mentioned in [44], the long-term component of PAL spectrum (τ_3, I_3) arises from the decay of the *o-Ps* triplet state in free-volume nanovoids of materials. The fitting parameters and positron trapping modes obtained at divided of PAL spectra for $(CsCl)_0$, $(CsCl)_5$, $(CsCl)_{10}$, and $(CsCl)_{15}$ glasses into three components are shown in Fig. 3.

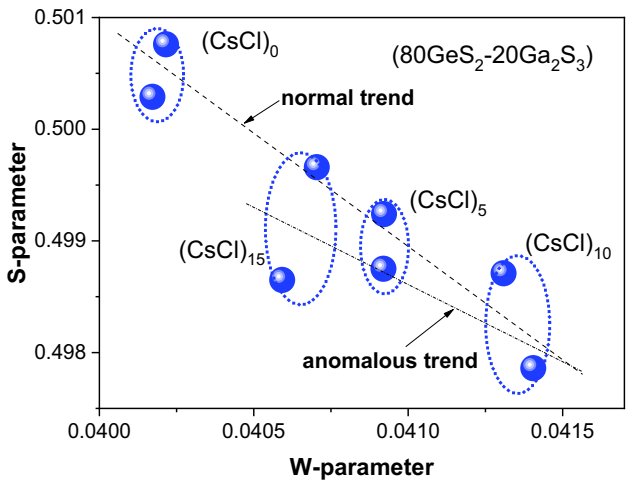

Fig. 2 *S*–*W* plots for the $80GeS_2$–$20Ga_2S_3$–CsCl glasses

Despite the low value of the intensity I_3 of the third component, its presence makes it possible to additionally estimate the size of the nanovoids. When the content of CsCl increases, the lifetime τ_3 increases. This indicates rise in the size of nanovoids (where the decay of o-Ps atoms occurs), while their number decreases simultaneously.

Changes in the parameters of the second defect-related (τ_2, I_2) component of the PAL spectrum correlate with the changes obtained with the two-component fitting procedure and reflect the agglomeration of internal free-volume defects when CsCl is added to the main GeS_2–Ga_2S_3 matrix (Fig. 3). The parameters of the second component for $(CsCl)_{15}$ show deviations from the revealed trend. Agglomeration of voids occurs in such glasses compared to basic samples, but compared to $(CsCl)_{10}$ glasses the size of free-volume defects decreases. In addition, the breakdown of the PAL spectrum into three components made it possible to detect another process that takes place in $(CsCl)_{15}$ glasses. An increase in the intensity of the third component I_3 and a decrease in the intensity of the second component I_2, as well as the value of τ_3 lifetime (which is similar to the annihilation of o-Ps in water bubbles [42]), indicate the annihilation of o-Ps in adsorbed water in this sample. A schematic illustration of the evolution of voids in Ge–Ga–S–CsCl glasses is shown in Fig. 4.

In the traditional mixed positron trapping and o-Ps decaying all studied glasses show close values of lifetimes τ_{av} and τ_b (Fig. 3). Such a high value of τ_b indicates a dense packing of the structure of glasses, which is caused by the fundamental impossibility of separating the contribution from the components associated with the positron trapping and o-Ps decaying. Other parameters of positron trapping modes are correlated to those obtained by decomposition into two components, which indicates the reproducibility of the research results and the correctness of the performed experiments.

In addition, using the lifetime of the third component τ_3 it was possible to calculate the radii of the nanovoids, where the processes of o-Ps decay occur according to the Tao–Eldrup model into spherical approximations [46, 47]. The obtained results are shown in Fig. 5.

At increasing of CsCl content agglomeration of nanovoids occurs for samples $(CsCl)_5$ and $(CsCl)_{10}$. However, a further increase in CsCl demonstrates an increase in the size of nanovoids and an increase in

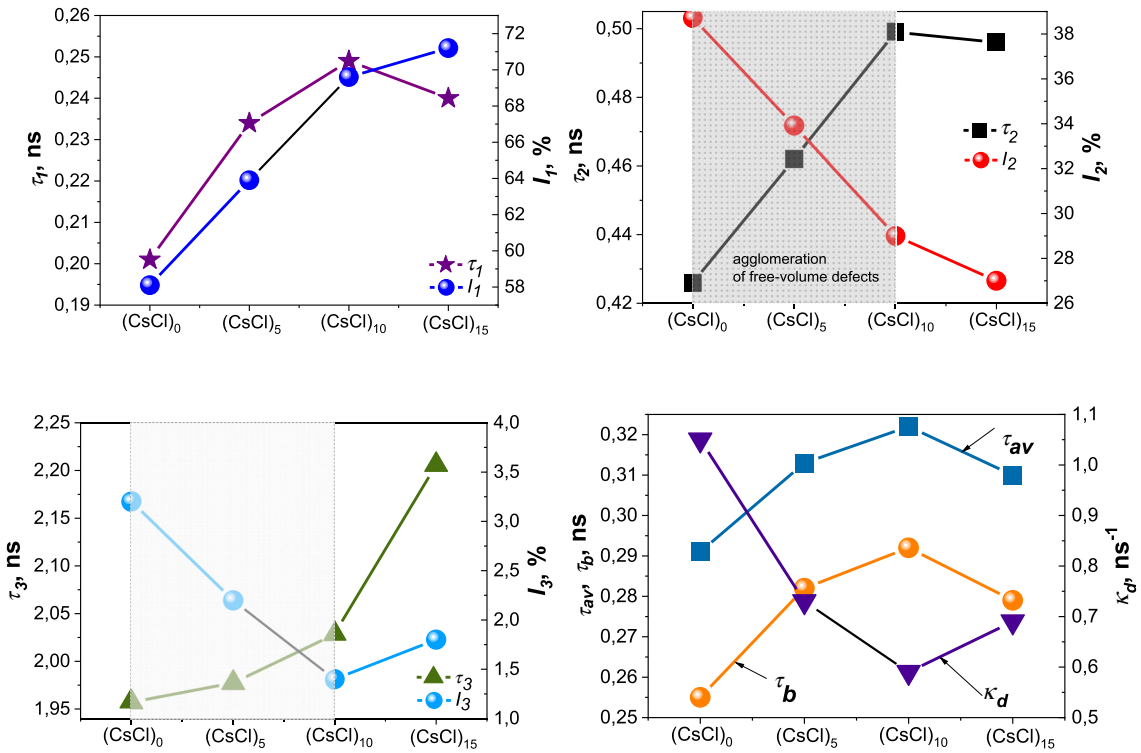

Fig. 3 Dependences of fitting parameters and positron trapping modes for the $80GeS_2–20Ga_2S_3–CsCl$ glasses calculated within three-components fitting procedure

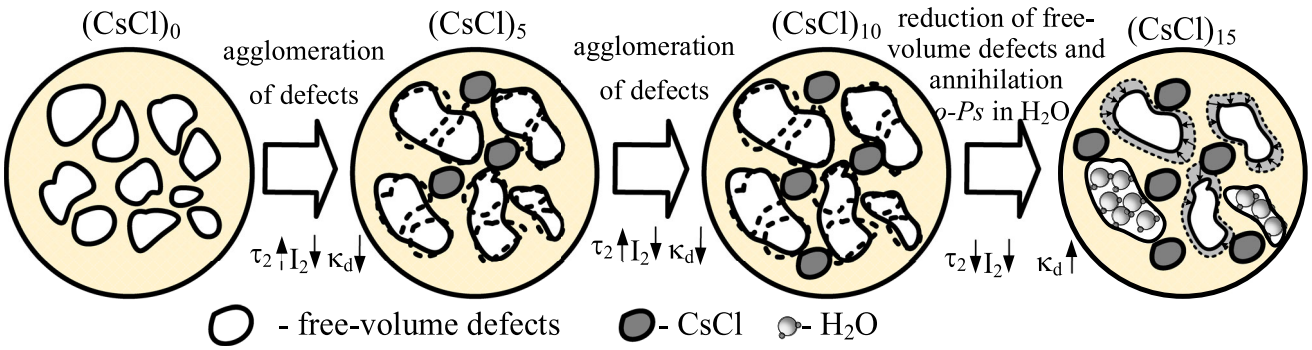

Fig. 4 Schematic image of modification of free-volume defects in the $80GeS_2–20Ga_2S_3–CsCl$ glasses

their number [for $(CsCl)_{15}$] compared to $(CsCl)_{10}$, which further confirms the anomalous processes in $(CsCl)_{15}$ glasses.

4 Conclusion

Changes in the structure of the internal positron trapping free-volume defects of $GeS_2–Ga_2S_3$ glasses due to the addition of different amounts of CsCl were studied. The PAL spectra were analyzed by decomposition into two and three components, which are correlated with each other. It is shown that an increase in the content of CsCl causes agglomeration of free-volume defects, which is reflected in an increase in the lifetime of the second component τ_2 and a decrease in the intensity I_2. Concentration of these defects is the subject of the most significant changes in composition changes and manifested in the positron trapping rate in defects κ_d. However, in the $(CsCl)_{15}$ sample there is a decrease in the size and content of these defects. The revealed trend correlates

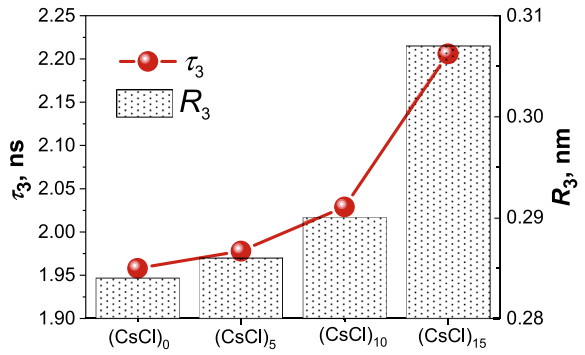

Fig. 5 Dependences of lifetime τ_3 and nanopores radius R_3 calculated within to Tao–Eldrup model for the studied $80GeS_2$–$20Ga_2S_3$–CsCl glasses

with the results of DRAL studies. The decomposition of PAL spectra into three components demonstrated that there is a certain amount of adsorbed water in $(CsCl)_{15}$ glasses. These changes were reflected in the lifetimes and intensities of the third component (τ_3, I_3), which is responsible for the decomposition of *o-Ps* atoms in nanopores and annihilation in water.

Acknowledgements

HK would like to thanks Ministry of Education and Science of Ukraine (Project No. 0122U000807) as well as Dr. A. Ingram for assistance in PAL and DRAL experiments and Prof. O. Spotyuk for discussions. In addition, the research of AIP was partly supported by the RADON project (GA 872494) within the H2020-MSCA-RISE-2019 call and COST Action CA20129 "Multiscale Irradiation and Chemistry Driven Processes and Related Technologies" (MultIChem). AIP also thanks to the Institute of Solid-State Physics, University of Latvia. ISSP UL as the Center of Excellence is supported through the Framework Program for European universities, Union Horizon 2020, H2020-WIDESPREAD-01-2016-2017-TeamingPhase2, under Grant Agreement No. 739508, CAMART2 project.

Author contributions

All authors contributed to the study conception and design. Glasses preparation was performed by LC Investigation, data collection and analysis were performed by HK and AIP. The first draft of the manuscript was written by HK and authors commented on the previous version of the manuscript. Authors read and approved the final manuscript.

Funding

The authors have not disclosed any funding.

Data availability

The datasets generated and analyzed during the current study are available from the corresponding author on reasonable request.

Declarations

Conflict of interest The authors declare no conflict of interest.

References

1. J.L. Adam, L. Calvez, J. Trolès, V. Nazabal, Chalcogenide glasses for infrared photonics. Int. J. Appl. Glass Sci. **6**(3), 287–294 (2015). https://doi.org/10.1111/ijag.12136
2. V. Nazabal, J.L. Adam, Infrared luminescence of chalcogenide glasses doped with rare earth ions and their potential applications. Opt. Mater. X **15**, 100168 (2022). https://doi.org/10.1016/j.omx.2022.100168
3. P. Lucas, Z. Yang, M.K. Fah, T. Luo, S. Jiang, C. Boussard-Pledel et al., Telluride glasses for far infrared photonic applications. Opt. Mater. Express **3**(8), 1049–1058 (2013). https://doi.org/10.1364/OME.3.001049
4. P. Patra, K. Annapurna, Transparent tellurite glass-ceramics for photonics applications: a comprehensive review on crystalline phases and crystallization mechanisms. Prog. Mater. Sci. **125**, 100890 (2022). https://doi.org/10.1016/j.pmatsci.2021.100890
5. W.A. Pisarski, Rare earth doped glasses/ceramics: synthesis, structure, properties and their optical applications. Materials **15**(22), 8099 (2022). https://doi.org/10.3390/ma15228099
6. B. Liu, Y. Mo, Y. Liu, Y. Lu, X. He, Y. Xu et al., Effects of alkali metal ion on imprinting GRIN microstructure in GeS_2-Ga_2S_3-MCl (M = na, K, Cs) glasses for visible to mid-infrared microgratings. Ceram. Int. **48**(22), 33122–33134 (2022). https://doi.org/10.1016/j.infrared.2022.104086
7. K. Hosoya, Y. Tokuda, A. Okada, T. Wakasugi, K. Kadono, Preparation, properties, and photodoping behavior of GeS_2-, Ga_2S_3-, and Sb_2S_3-based glasses with excess sulfur and CsCl.

J. Mater. Res. **34**(16), 2747–2756 (2019). https://doi.org/10.1557/jmr.2019.209

8. H. Tao, G. Dong, Y. Zhai, H. Guo, X. Zhao, Z. Wang, Q. Gong, Femtosecond third-order optical nonlinearity of the GeS_2-Ga_2S_3-CdI_2 new chalcohalide glasses. Solid State Commun. **138**(10–11), 485–488 (2006). https://doi.org/10.1016/j.ssc.2004.02.046
9. H. Guo, Y. Zhai, H. Tao, Y. Gong, X. Zhao, Synthesis and properties of GeS_2–Ga_2S_3–PbI_2 chalcohalide glasses. Mater. Res. Bull. **42**(6), 1111–1118 (2007). https://doi.org/10.1016/j.materresbull.2006.09.007
10. S.V. Luniov, A.I. Zimych, P.F. Nazarchuk, V.T. Maslyuk, I.G. Megela, Radiation defects parameters determinationin n-Ge single crystals irradiated by high-energy electrons. Nuclear Phys. Atomic Energy **17**(1), 47–52 (2016). https://doi.org/10.15407/jnpae2016.01.047
11. I. Kebaili, I. Boukhris, Z.A. Alrowaili, M.M. Abutalib, M.S. Al-Buriahi, Characterization of physicochemical properties of As_2Se_3–GeTe–AgI chalcohalide glasses for solar cell and IR applications: influence of adding AgI. J. Mater. Sci. Mater. Electron. **33**(2), 800–809 (2022). https://doi.org/10.1007/s10854-021-07350-y
12. G. Dong, H. Tao, X. Xiao, C. Lin, X. Zhao, S. Gu, Study of thermal and optical properties of GeS_2–Ga_2S_3–Ag_2S chalcogenide glasses. Mater. Res. Bull. **42**(10), 1804–1810 (2007). https://doi.org/10.1016/j.materresbull.2006.12.003
13. W. Xu, D. Chen, Q. Yan, J. Ren, G. Chen, Silver metal enhanced photoluminescence of Tm^{3+} doped GeS_2–Ga_2S_3–CsCl glasses. J. Non-Cryst. Solids **358**(23), 3065–3068 (2012). https://doi.org/10.1016/j.jnoncrysol.2012.08.009
14. C. Li, H. Liu, G. Zhou, S. Kang, L. Tan, C. Gao, C. Lin, Infrared GRIN GeS_2–Sb_2S_3–CsCl chalcogenide glass–ceramics. J. Am. Ceram. Soc. **105**(10), 6007–6012 (2022). https://doi.org/10.1111/jace.18598
15. M. Li, Y. Xu, X. Jia, L. Yang, N. Long, Z. Liu, S. Dai, Mid-infrared emission properties of Pr^{3+}-doped Ge-Sb-Se-Ga-I chalcogenide glasses. Opt. Mater. Express **8**(4), 992–1000 (2018). https://doi.org/10.1364/OME.8.000992
16. X. Shen, F. Chen, X. Lv, S. Dai, X. Wang, W. Zhang et al., Preparation and third-order optical nonlinearity of glass ceramics based on GeS_2–Ga_2S_3–CsCl pseudo-ternary system. J. Non-Cryst. Solids **357**(11–13), 2316–2319 (2011). https://doi.org/10.1016/j.jnoncrysol.2011.01.019
17. G. Yang, C. Yang, D. Hu, C. Peng, K. Tang, Y. Lu et al., Effect of halogen on imprinting gradient refractive index microstructure in GeS_2–Ga_2S_3–NaX (X = F, Cl, br, I) glasses for broadband infrared diffraction gratings. Ceram. Int. **47**(20), 28511–28520 (2021). https://doi.org/10.1016/j.ceramint.2021.07.008
18. Y. Zhang, Q. Jiao, B. Ma, C. Lin, X. Liu, S. Dai, Structure and ionic conductivity of new Ga_2S_3-Sb_2S_3-NaI chalcogenide glass system. Physica B **570**, 53–57 (2019). https://doi.org/10.1016/j.physb.2019.05.026
19. Q. Yan, Y. Liu, W. Wang, G. Chen, Luminescence behaviors of the Eu^{2+} ions in the GeS_2-Ga_2S_3-CsCl chalcohalide glasses. J. Non-Cryst. Solids **357**(11–13), 2472–2474 (2011). https://doi.org/10.1016/j.jnoncrysol.2010.11.054
20. H. Klym, I. Karbovnyk, M.C. Guidi, O. Hotra, A.I. Popov, Optical and vibrational spectra of CsCl-enriched GeS_2-Ga_2S_3 glasses. Nanoscale Res. Lett. **11**(1), 1–6 (2016). https://doi.org/10.1186/s11671-016-1350-8
21. A. Kozlovskiy, D.I. Shlimas, M.V. Zdorovets, E. Popova, E. Elsts, A.I. Popov, Investigation of the efficiency of shielding gamma and electron radiation using glasses based on TeO_2-WO_3-Bi_2O_3-MoO_3-SiO to protect electronic circuits from the negative effects of ionizing radiation. Materials **15**(17), 6071 (2022). https://doi.org/10.3390/ma15176071
22. K. Tanaka, A. Saitoh, Pulsed light effects in amorphous As_2S_3. J. Mater. Sci. Mater. Electron. **33**, 22029–22052 (2022). https://doi.org/10.1007/s10854-022-08989-x
23. I. Hadzaman, H. Klym, O. Shpotuyk, M. Brunner, Temperature sensitive spinel-type ceramics in thick-film multilayer performance for environment sensors. Acta Phys. Polonica-Series Gen. Phys. **117**(1), 234 (2010)
24. V.P. Savchyn, A.I. Popov, O.I. Aksimentyeva, H. Klym, Y.Y. Horbenko, V. Serga et al., Cathodoluminescence characterization of polystyrene-$BaZrO_3$ hybrid composites. Low Temp. Phys. **42**(7), 597–600 (2016). https://doi.org/10.1063/1.4959020
25. V.V. Halyan, V.O. Yukhymchuk, Y.G. Gule, I.V. Kityk, Y. Zhydachevskyy, I.A. Ivashchenko et al., Specific features of stokes photoluminescence of the La_2S_3–Ga_2S_3–Er_2S_3 glasses. Opt. Mater. **128**, 112394 (2022). https://doi.org/10.1016/j.optmat.2022.112394
26. P. Naresh, M. Kostrzewa, M.G. Brik, A.S.S. Reddy, N.K. Mohan, V.R. Kumar et al., Nd^{3+}-Doped lead boro selenate glass: a new efficient system for near-infrared 1.06 μm laser emission. Phys. Status Solidi (a) **217**(24), 2000602 (2020). https://doi.org/10.1002/pssa.202000602
27. R. Golubevas, A. Zarkov, L. Alinauskas, Z. Stankeviciute, G. Balciunas, E. Garskaite, A. Kareiva, Fabrication and investigation of high-quality glass-ceramic (GC)–polymethyl methacrylate (PMMA) composite for regenerative medicine. RSC Adv. **7**(53), 33558–33567 (2017). https://doi.org/10.1039/C7RA05188C
28. U. Rogulis, E. Elsts, J. Jansons, A. Sarakovskis, G. Doke, A. Stunda, K. Smits, Cathodoluminescence of oxyfluoride glass-ceramics. Radiat. Meas. **56**, 120–123 (2013). https://doi.org/10.1016/j.radmeas.2012.12.020

29. P.V. Savchyn, V.V. Vistovskyy, A.S. Pushak, A.S. Voloshinovskii, A.V. Gektin, V. Pankratov, A.I. Popov, Synchrotron radiation studies on luminescence of Eu^{2+}-doped $LaCl_3$ microcrystals embedded in a NaCl matrix. Nuclear Instrum. Methods Phys. Res. Section B **274**, 78–82 (2012). https://doi.org/10.1016/j.nimb.2011.11.024
30. S.V. Luniov, A.I. Zimych, P.F. Nazarchuk, V.T. Maslyuk, I.G. Megela, The impact of radiation defects on the mechanisms of electron scattering in single crystals n-Ge. J. Phys. Stud. **19**(4), 4704–4704 (2015). https://doi.org/10.30970/jps.19.4704
31. A.L. Kozlovskiy, A.S. Seitbayev, D.B. Borgekov, M.V. Zdorovets, Study of the structural, optical and strength properties of glass-like (1 – x)ZnO–0.25Al_2O_3–0.25 WO_3–xBi_2O_3 Ceramics. Cryst. **12**(11), 1527 (2022). https://doi.org/10.3390/cryst12111527
32. A.V. Fedosov, S.V. Luniov, S.A. Fedosov, Specific features of intervalley scattering of charge carriers in n-Si at high temperatures. Semicond. **44**, 1263–1265 (2010). https://doi.org/10.1134/S1063782610100039
33. L.H. Cong, B.C. Gu, X.X. Han, Q.H. Zhao, Z.W. Pan, R. Ye et al., Reconfigurable positron annihilation lifetime spectrometer utilizing a multi-channel digitizer. Nuclear Instrum. Methods Phys. Res. Section A (2019). https://doi.org/10.1134/S1063782610100039
34. W.J. Legerstee, T. Noort, T.K. van Vliet, H. Schut, E.M. Kelder, Characterisation of defects in porous silicon as an anode material using positron annihilation doppler broadening spectroscopy. Appl. Nanosci. **12**(11), 3399–3408 (2022). https://doi.org/10.1007/s13204-022-02550-2
35. H. Klym, L. Calvez, A.I. Popov, Free-volume extended defects in structurally modified Ge–Ga–S/Se glasses. Phys. Status Solidi (b) **259**(8), 2100472 (2022). https://doi.org/10.1002/pssb.202100472
36. H. Klym, A.D.A.M. Ingram, O. Shpotyuk, Free-volume nanostructural transformation in crystallized GeS2–Ga2S3–CsCl glasses. Materialwiss. Werkstofftech. **47**(2–3), 198–202 (2016). https://doi.org/10.1002/mawe.201600476
37. H. Klym, A. Ingram, O. Shpotyuk, I. Karbovnyk, Influence of CsCl addition on the nanostructured voids and optical properties of 80GeS_2-20Ga_2S_3 glasses. Opt. Mater. **59**, 39–42 (2016). https://doi.org/10.1016/j.optmat.2016.03.004
38. H. Klym, A. Ingram, O. Shpotyuk, O. Hotra, A.I. Popov, Positron trapping defects in free-volume investigation of Ge–Ga–S–CsCl glasses. Radiat. Meas. **90**, 117–121 (2016). https://doi.org/10.1016/j.radmeas.2016.01.023
39. P. Masselin, D. Le Coq, L. Calvez, E. Petracovschi, E. Lépine, E. Bychkov, X. Zhang, CsCl effect on the optical properties of the 80GeS_2–20Ga_2S_3 base glass. Appl. Phys. A **106**(3), 697–702 (2012). https://doi.org/10.1007/s00339-011-6668-6
40. Y. Ledemi, L. Calvez, M. Rozé, X.H. Zhang, B. Bureau, M. Poulain, Y. Messaddeq, Totally visible transparent chlorosulphide glasses based on Ga_2S_3-GeS_2-CsCl. J. Optoelectron. Adv. Mater. **9**(12), 3751 (2007)
41. H. Kalman, D. Portnikov, Analyzing bulk density and void fraction: A the effect of archimedes number. Powder Technol. **381**, 477–487 (2021). https://doi.org/10.1016/j.powtec.2020.12.014
42. R. Golovchak, A. Kozdras, S. Kozyukhin, O. Shpotyuk, High-energy γ-irradiation effect on physical ageing in Ge–Se glasses. Nucl. Instrum. Methods Phys. Res. Section B **267**(17), 2958–2961 (2009). https://doi.org/10.1016/j.nimb.2009.06.011
43. D. Giebel, J. Kansy, LT10 program for solving basic problems connected with defect detection. Phys. Procedia **35**, 122–127 (2012). https://doi.org/10.1016/j.phpro.2012.06.022
44. H. Klym, I. Karbovnyk, S. Piskunov, A.I. Popov, Positron annihilation lifetime spectroscopy insight on free volume conversion of nanostructured $MgAl_2O_4$ ceramics. Nanomaterials **11**(12), 3373 (2021). https://doi.org/10.3390/nano11123373
45. H. Klym, A. Ingram, O. Shpotyuk, R. Szatanik, Free-volume study in GeS_2-Ga_2S_3-CsCl chalcohalide glasses using positron annihilation technique. Phys. Procedia **76**, 145–148 (2015). https://doi.org/10.1016/j.phpro.2015.10.026
46. S. Thraenert, E.M. Hassan, D. Enke, D. Fuerst, R. Krause-Rehberg, Verifying the RTE model: ortho-positronium lifetime measurement on controlled pore glasses. Phys. Status Solidi C **4**(10), 3819–3822 (2007). https://doi.org/10.1002/pssc.200675738
47. R. Zaleski, J. Wawryszczuk, T. Goworek, Pick-off models in the studies of mesoporous silica MCM-41. Comparison of various methods of the PAL spectra analysis. Radiat. Phys. Chem. **76**(2), 243–247 (2007). https://doi.org/10.1016/j.radphyschem.2006.03.044